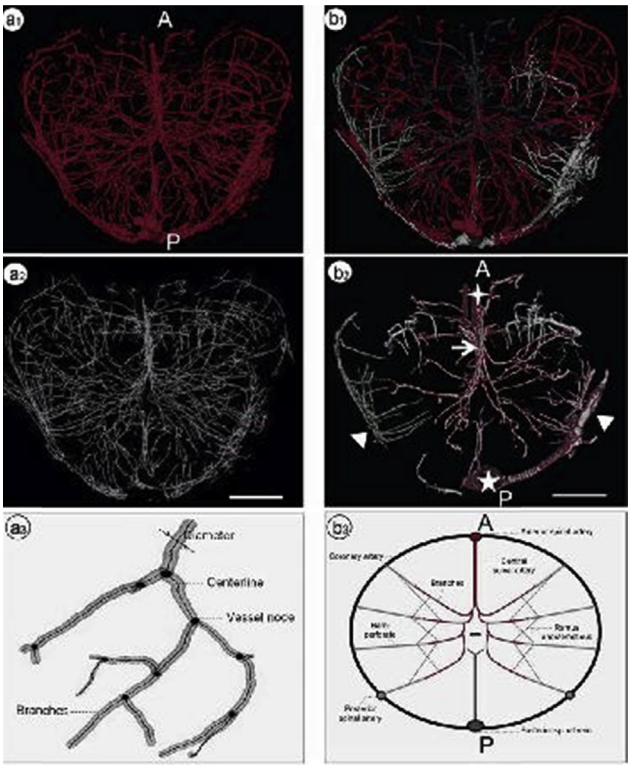

Fig. 1 (a) Synchrotron radiation image optimization, (a1) The whole 3D volumetric rendering of the intact vasculature of the normal spinal cord segment. (a2) The centraxonial vessel skeleton was abstracted from the 3D spatial angioarchitecture. (a3) The illustration to characterize the vascular branch feature with a simulative analytical model. Fig. 2 (b) Vascular arrangement of blood supply in spinal cord. (b1-2) The pseudocolors were painted to display the different administrative region from the top view. (cross=ASA; triangle=PSA; arrow=CSA; star=PSV; ba=500 μ m) (b3). A manual drawing to simulate the blood supply pattern of rat normal spinal cord. (A=anterior; P=posterior).

IBDW2014-00155-F0076
A NOVEL STUDY BY CONFOCAL RAMAN MICRO-SPECTROSCOPY IN THE RABBIT BONE-TENDON JUNCTION OF THE PATELLA-PATELLAR TENDON

Zhanwen Wang, Ziteng Zeng, Cheng Zheng, Jingyong Zhou, Jianzhong Hu, Hongbin Lu
Department of Sports Medicine and Research Center of Sports Medicine, Xiangya Hospital, Central South University, Changsha, PR China

Objective: With confocal Raman micro-spectroscopy, we tried to distinguish different structures of rabbit patellar-patellar tendon junction (PPT) and explore the new method for further study to evaluate bone tendon junction healing.
Methods: The PPT samples were harvested carefully from four healthy bone matured male New Zealand rabbits cadavers and were sectioned crossing the median sagittal plane. All samples underwent no chemical treatment for Raman analysis. After all the Raman spectra were acquired, baseline correction for each individual spectrum was performed. The relative peak intensity of 960Δcm-1 standing for mineral and 2940Δcm-1 for collagen as well as mineral-to-collagen ratio (960Δcm−1/2940Δcm- 1) was used as indicators to identify which structure the scanning spot belongs to. Meanwhile, through X-axis coordinate of each individual position, the thickness of the junction in rabbit PPT can be calculated. After Raman spectroscopy scanning, the PPT samples were observed optically in histological sections (HE staining).
Results: According to Raman analysis, three different yet continuous structures of PPT could be well identified: bone, fibrocartilage, and tendon (Fig 1A). The thickness of fibrocartilage was about 1800μm. This result was highly consistent with histological study. The collagen content (the peak intensity strength of 2940Δcm-1) in bone was higher than tendon (Fig 1A). We also found that the mineral-to-collagen ratio gradually increased across the junction from the tendon to bone. The 960Δcm-1 band across the junction became narrow in the same mineral zone. Interestingly, we found that combined with histological observation, some scanning spots around the tidemark showed higher mineral-to-collagen ratio than bone (Fig 1B). This might be the result of the process of continuous and dynamic mineralization existing around the boundary (i.e., tidemark) region.
Conclusion: Confocal Raman micro-spectroscopy could be used to distinguish and measure the thickness of the classic structures of the PPT samples. Furthermore, it could detect the distribution and the degree of mineralization as well as the content of the organic tissue (almost collagen I) across the tendon—bone junction.
Acknowledgement
This work was supported by The National Natural Science Foundation of China (No. 81171699).
B: Mineral/Collagen Ratio of each spectrum in A.

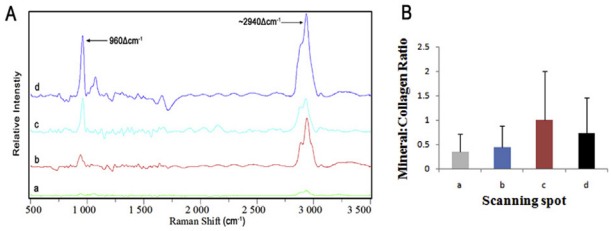

Fig. 1. A: The classical spectra of sample #2. Spectrum ***a*** represented for tendon, ***b&c*** for fibrocartilage and ***d*** for bone. The position of spectrum ***c*** was around the timemark. Mineralization increased from tendon to bone. The collagen content in bone was higher than tendon.

IBDW2014-00156-F0077
CHARACTERIZATION OF ZINC AND CALCIUM SPATIAL DISTRIBUTION AT THE FIBROCARTILAGE OF RABBIT PATELLA-PATELLAR TENDON COMPLEX: A SYNCHROTRON RADIATION MICRO X-RAY FLUORESCENCE STUDY

Can Chen [a], Zhanwen Wang [a], Cheng Zheng [a], Tianding Wu [b], Yong Cao [b], Hu Jianzhong [b], Yi Zheng [a,b], Hongbin Lu [a]
[a]*Department of Sports Medicine, Research Center of Sports Medicine, Xiangya Hospital, Central South University, Changsha, Hunan, PR China*
[b]*Department of Spine Surgery, Xiangya Hospital, Central South University, Changsha, Hunan, PR China*

Objective: Zinc (Zn) and calcium (Ca) play important roles in the normal growth, remodeling and mineralization of fibrocartilage zone of patella-patellar tendon complex (PPTC). Synchrotron radiation micro X-ray fluorescence (SR-μXRF) allows in situ mapping of Zn and Ca at nanometer level with high sensitivity. Therefore, the main purpose of this study was to characterize the distribution of Zn and Ca at the fibrocartilage zone of PPTC.
Methods: (1) Sample Preparation: Four PPTC of rabbits were embedded with polymethylmethacrylate and cut sagittally with a thickness of 100μm. (2) Backscattered electron imaging (BEI): An electron-probe microanalyzer was utilized to acquire BEI images. The region of interest and tidemark (TM) of PPTF were determined based on the BEI images (Fig.1.A). (3) SR-μXRF: the distribution of Zn and Ca at the fibrocartilage zone of PPTC were examined at BL15U1 (Shanghai Synchrotron Radiation Facility, China) and analyzed with Igor pro program (Version 6.1, WaveMetrics, Inc, USA).
Results: (1) The distribution of Zn and Ca at the fibrocartilage zone of PPTC was successfully visualized by using SR-μXRF. The spatial resolution of elemental mapping was as small as 3 μm (Fig. 1.B). (2) The distribution of Zn and Ca at the fibrocartilage zone of PPTC was inhomogeneous. The content of Zn in the TM zone was 2.8 times higher than that of patellar tendon (Fig.1.D) (Fig.2.D). The position of highest Ca content (21.9 times of that of patellar tendon) was located in the calcified fibrocartilage zone and is about 100μm far from where the highest Zn content is. Most importantly, Ca was distributed in a gradually decreasing manner from bone to tendon

(Fig.1.C) (Fig.2.D). Moreover, the ratios of Ca maximum and Zn maximum in PPTF were about 12.3(Fig.2.D).
Conclusion: SR-μXRF was able to accurately determine the distribution of Zn and Ca at the fibrocartilage zone of PPTC. The highest Ca position was different from where the highest Zn content is.

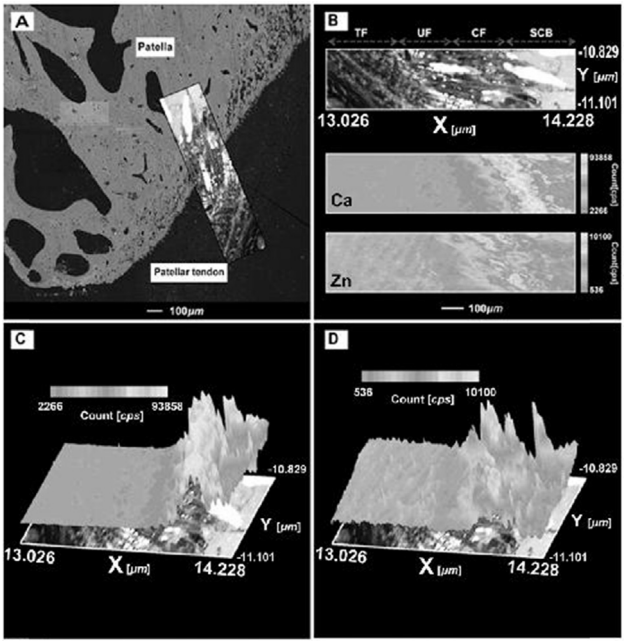

Fig.1. (A) Backscattered electron imaging of PPTC with a Van-Gieson staining image. Red dashed line showing the TM of PPTC. **(B)** Ca and Zn fuorescence mapping and corresponding Van-Gieson staining of PPTC. SCB(subchondral bone); CF(calcified fibrocartilage);UT (uncalcified fibrocartilage); TF (tendon fiber). **(C&D)** Distribution of Zn and Ca in PPTC. The fluorescence yield counts were normalized by 10 and dwell time. Color-coding scale bar of Zn and Ca was displayed at the right of each elemental mapping and represent the range of the colour map for each image.

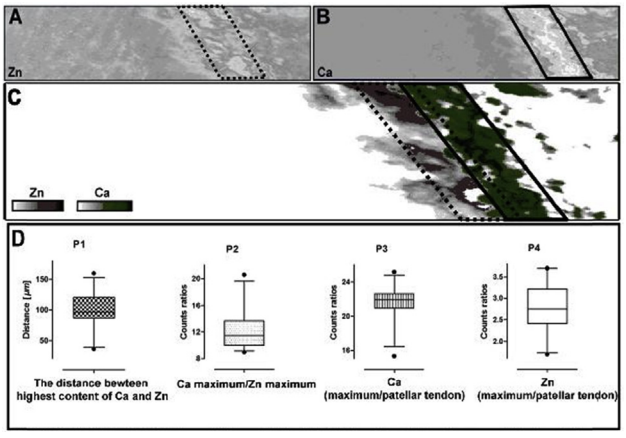

Fig.2. (A&B) The distributiona of Zn and Ca in PPTC. The black dashed box and black solid box respectively presented the accumulating region of Zn and Ca. **(C)** The difference of the highest content position of Zn and Ca. Red box: the highest content of Zn; Green box: the highest content of Ca. **(D)** Whisker plots showing Mean, 95% confidence interval for Mean(box) and range (error) bars) of Zn and Ca distribution. PI (distance between Zn and Ca maximum position); P2 (counts ratios of Ca and Zn maximum); P3 (Ca - counts ratios of maximum and patellar tendon);P4 (Zn - counts ratios of maximum and patellar tendon).

IBDW2014-00157-F0078
GLUCOCORTICOID BIDIRECTIONALLY REGULATE THE DIFFERENTIATION OF BONE MARROW STROMAL CELLS

Junling Wang, Simin Huang, Xin Tan, Qiushi Wei, Weimin Deng
Department of rehabilitation, general hospital of guangzhou military command of PLA, Guangzhou, China

Osteoporosis is a systemic metabolic disease which is characterized by a decrease in bone mass as well as a deterioration of the bone architecture. It leads to an increase in bone fragility and risk of a fracture. Glucocorticoid is widely used for their unsurpassed anti-inflammator and immunomodulatory effects. However, excess glucocorticoid will result in osteoporosis, one of the secondary osteoporosis. Bone marrow stromal cells (BMSCs) have the potential of multi-directional differentiation, from which adipocytes and osteoblasts are originated. Within the bone marrow, the differentiation into adipocytes or osteoblasts is competitively balanced. Glucocorticoids are widely used in clinic for their unsurpassed anti-inflammatory and immunomodulatory effects. However, it has been reported that excessive glucocorticoids could cause the outbreak of osteoporosis. In a certain range, glucocorticoids promote the osteogenic differentiation and adipogenic differentiation. Combination of glucocorticoids with many different factors can up-regulate or down-regulate osteogenic differentiation. This review summarized the two-way regulation to the BMSCs differentiation by glucocorticoid, further investigations on which factors can glucocorticoid combine with to promote the maximized osteogenic differentiation.

IBDW2014-00158-F0079
3D MICROARCHITECTURE QUANTIFICATION OF BONE REGENERATION DURING BONE-TENDON JUNCTION HEALING BY SR-μCT

Cheng Zheng [a,b], Zhanwen Wang [a], Can Chen [a], Jingyong Zhou [a], Jianzhong Hu [a], Hongbin Lu [a]
[a]*Department of Sports Medicine, Research Center of Sports Medicine, Xiangya Hospital, Central South University, Changsha, Hunan, PR China*
[b]*Sports Medicine & Rehabilitation Center, Wuhan Sports University, Wuhan, Hubei, PR China*

Objective: The aim of this study was to quantitatively evaluate microarchitecture of newly formed trabecular bone during healing process of bone-tendon junction (BTJ), and to explore the feasibility of application of synchrotron radiation micro computed tomography (SR-μCT) in 3D visualization of BTJ.
Methods: Six skeletal mature female New Zealand rabbits with partial patellectomy were used to establish a BTJ injury model, three patella-patellar tendon complexes were harvested at postoperative week 6 and 14, respectively, while three specimens were obtained in normal rabbits without surgery. Specimens were dehydrated followed by cut specimens along the sagittal. The x-ray phase contrast imaging experiments and image process were performed at X-ray imaging and biomedical application beamline (BL13W1) of Shanghai Synchrotron Radiation Facility in China. The projection images were captured by CCD detector with a 0.74 μm resolution. The 3D visualization images of BTJ were acquired and two region of interest (ROI) of newly formed trabecular bone in BTJ of each sample were analyzed.
Results: Due to the high resolution and sensibility of SR-μCT, the four layer structure of BTJ was distinguished with high resolution, such as bone, calcified fibrocartilage, uncalcified fibrocartilage, and tendon (Fig 1). Compared with normal trabecular bone, the new trabecular bone showed significantly lower BV/TV, Tb.Sp and Tb.Th, and significantly higher Tb.N at postoperative week 6. While at week 14, the BV/TV and Tb.N of the new trabecular bone were significantly lower than that of normal trabecular bone, the Tb.Sp and Tb.Th were significantly higher in the new trabecular bone. The BV/TV, Tb.Sp and Tb.Th were found to increase from week 6 to week 14, while the Tb.N decreased from week 6 to week 14 (Fig 2). The changes of these parameters reflect the remolding of new trabecular bone during healing process.
Conclusion: The newly formed trabecular bone of BTJ gradually remolding during the healing process and the SR-μCT can be applied for 3D visualization and quantitatively evaluating the microarchitecture of new bone in BTJ healing.
Acknowledgement
This work was supported by the National Natural Science Foundation of China (No. 81171699). We acknowledge the X-ray imaging and biomedical application beamline of Shanghai Synchrotron Radiation Facility in China on the SR-μCT experiments and image process.